Chapter 4

FAULT EVENTS CLASSIFICATION USING EMD & MACHINE LEARNING TECHNIQUES

4.1 Introduction

This chapter describes the EMD and non-parametric ML based methodology for identifying the fault events in the compensated power transmission network. The basic work-flow of the proposed fault ascertaining scheme is shown in Figure 4.1. Here also the similar idea of feature extraction based fault detection mechanism has been utilized. But instead of DWT, empirical mode decomposition mechanism has been employed for extracting the fault feature vectors. The application of EMD mechanism instead of DWT technique outperforms the critical limitations associated with DWT based signal decomposition. The DWT decomposition usually involves concerns like selection of reasonable mother wavelet and level decomposition. The precision of signal analysis while using DWT is incumbent on the selection the mother wavelet according to the symmetry of the original signal. Contrarily, the EMD based signal decomposition is totally free from picking of predefined mother mathematical function as in the DWT. The fault characteristics feature extracted after EMD decomposition are fed to the ML classifier models for identifying the particular fault events in the network. The training and testing mechanism of the proposed EMD based scheme is thoroughly described in this chapter. Further, the strength and workability of the proposed EMD and ML based scheme is analyzed in the simulated test networks for various fault scenarios.

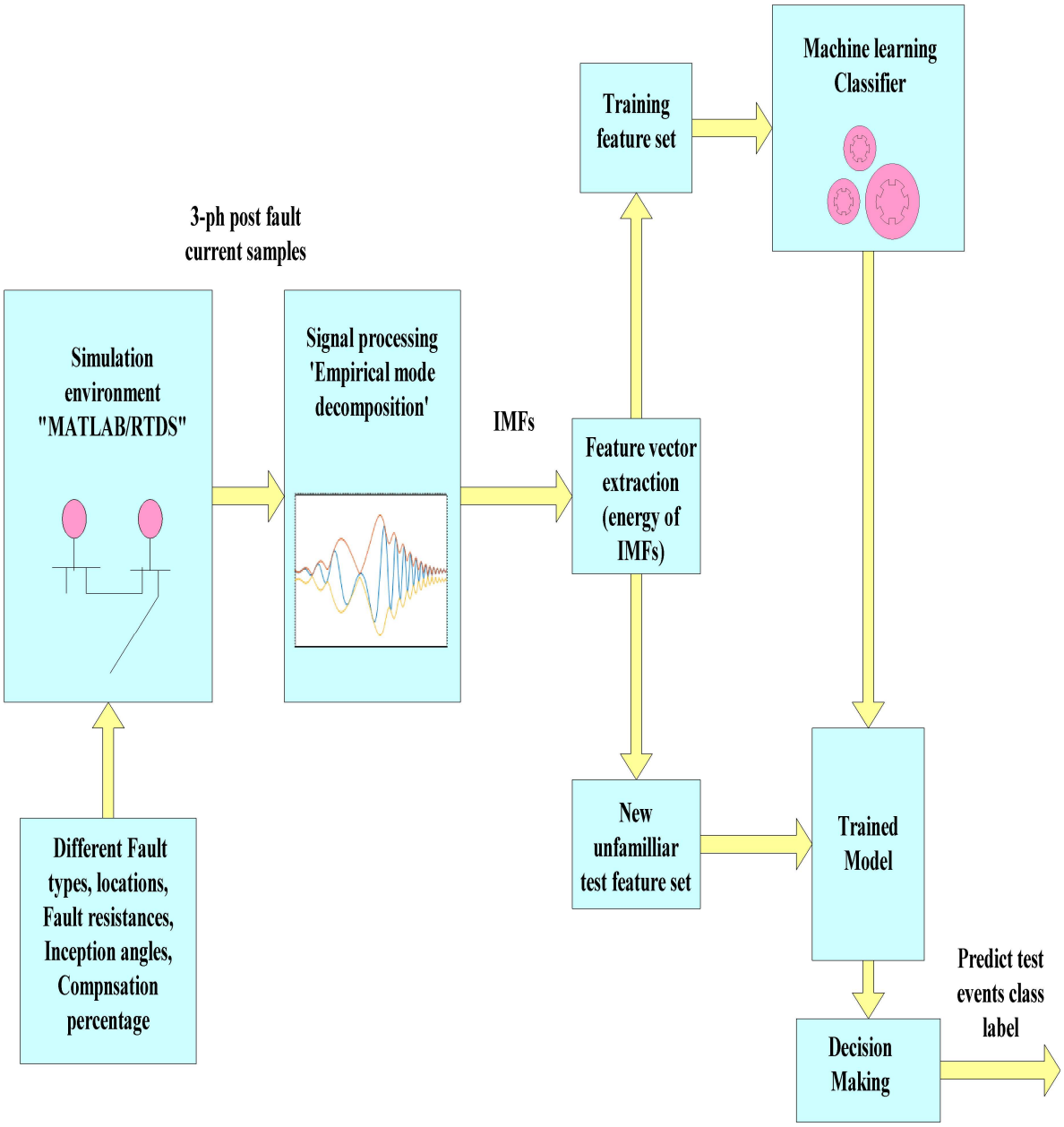

Figure 4.1 Structure of EMD and ML based events classification scheme

4.2 Proposed EMD and Non-parametric ML based Fault Events Classification Scheme

In the present scheme, in lieu of DWT the empirical mode signal decomposition mechanism has been utilized for processing the post fault current samples as it offers more versatility and has large extent of adaptation in comparison to other techniques like FT, STFT or wavelet transforms. The retrieved post fault current samples are decomposed into different IMFs using EMD technique. The principle and procedures of EMD technique has been already discussed in section 2.5. Once the intrinsic mode function (IMFs) have been obtained the fast Fourier transform (FFT) mechanism has been applied on acquired IMFs for identifying the desirable IMFs which is having similar transient frequency range. After identifying the desirable IMFs, the fault characteristic features for each phase (i.e. E_a, E~~b~~, and E_c) are computed in terms of its energy level as discussed in section 2.6.2. Finally, the computed energy based feature vectors are employed as training and testing samples to the designed ML classifier models for identifying the particular events in the transmission network. The classifier model forecast the individual category of the test instance as its output on the basis of learned pattern during training. The flowchart of the proposed EMD and ML based fault events classification scheme is shown in Figure 4.2.

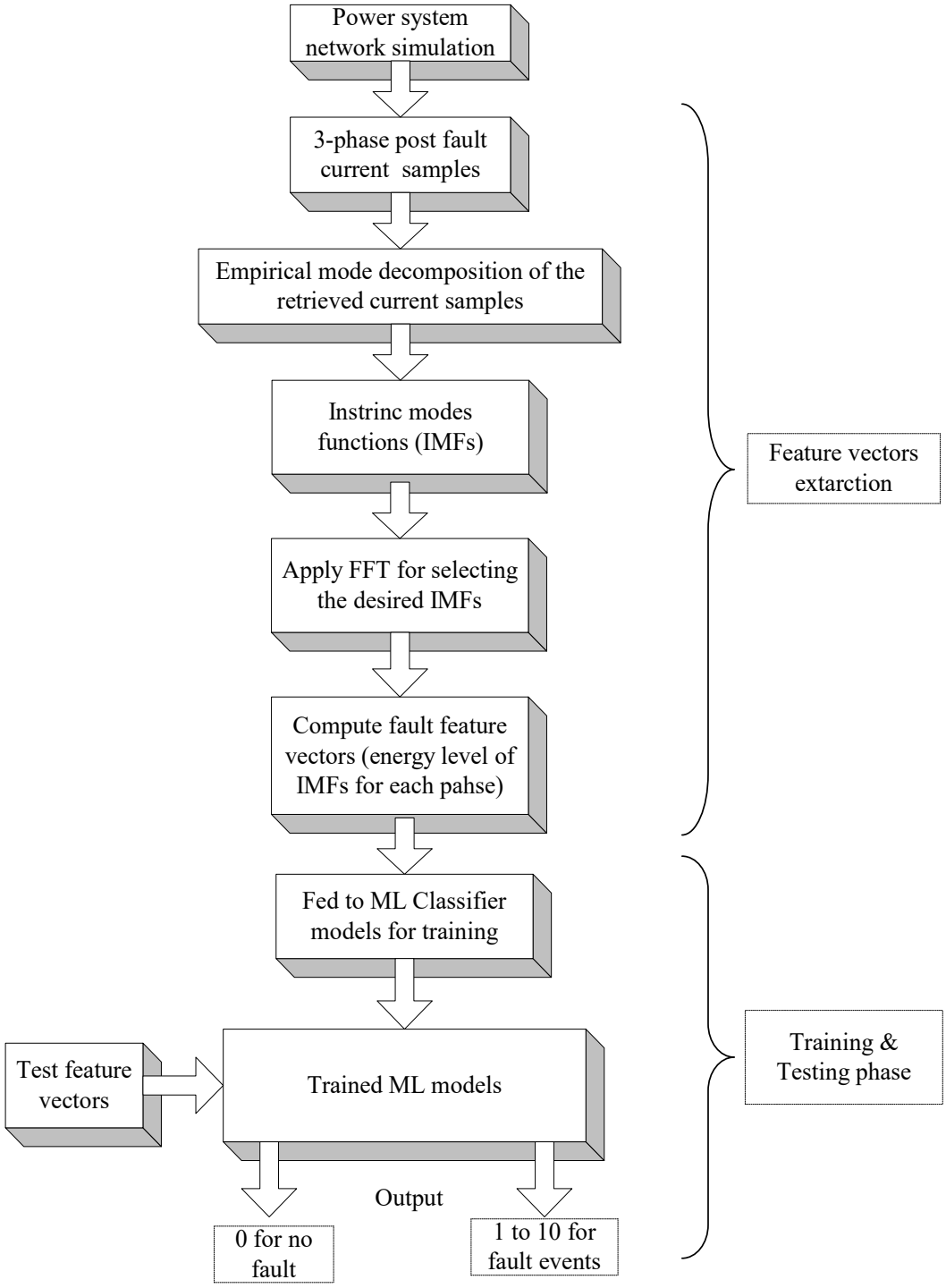

Figure 4.2 Work-flow of the proposed fault events classification scheme

4.2.1 Training and Testing Mechanism

The same ML classifier models i.e. K-NN, SVM, and PNN have been utilized in this methodology for identifying the fault events in the transmission network. For training the classifier models, the computed feature vectors in terms of the energy of desired IMFs i.e. (E_a, E~~b~~, and E_c) corresponding to different scenarios such as normal operating mode and during fault conditions with varying fault types, location of faults, fault resistances, inception angles and percentage of line compensation are applied to the classifier models. Different fault events in the transmission circuit are labelled in the following manner: no fault- class 0, AG-class1, BG-class 2, CG-class 3, AB-class 4, AC-class 5, BC-class 6, ABG-class 7, BCG-class 8, ACG-class 9, ABC-class 10. Once the training feature samples of each phase are applied to the individual classifier model, it start recognizing and learning the features pattern associated with different fault scenarios by using its computing algorithms. For evaluating the feasibility and efficiency of the proposed EMD and ML based scheme, multiple unfamiliar fault cases as stated in Table 4.1 have been considered for testing. The utilized test samples comprises of feature vectors associated with 10 normal operating cases and new fault cases at 7 different locations in the network, with changing fault resistances (6), fault inceptions angles (6), two level of line compensation. During the training phase, the classifier models become well capable of predicting the class label of the unfamiliar test cases on the basis of learned pattern set. Afterwards, during the validation phase of the proposed scheme the extracted feature vectors associated with multiple considered test cases are applied as input to the trained ML classifier models. The models compare the test dataset with the learned pattern set during training and accordingly make the decision regarding the particular class label of the test case as its output.

4.3 Case Study and Results

For vindicating the capability of the proposed EMD and ML based fault events categorization scheme, it has been examined for various fault scenarios in the simulated test networks. It has been considerably tested for all sorts of shunt fault events and evolving fault events in the transmission circuit. The details of training and testing cases and varying conditions considered on the first simulated test network are listed in Table 4.1. The ML classifier models compute the distance of the test feature set with the trained pattern set and on that basis it predicts the particular category of the test case.

Table 4.1 Training and testing condition considered on first test system

S. No	Parameters	Training cases	Testing cases
1.	Fault locations (km)	Twenty different locations	Seven new unknown location (30 km, 50km, 110 km, 170 km, 190 km, 230 km and 250 km)
2.	Fault Resistance (ohms)	0.001, 20, 60	0.1, 0.5, 1, 5, 10, 50
3.	Fault inception angle (°)	0, 75, 150	30, 45, 60, 90, 120, 135
4.	Fault events types	No fault and all kinds faults events	Unknown no fault and all kinds of fault events
5.	Level of line compensation	35 % and 45 %	30 % and 40 %

4.3.1 Test case 1: Two-bus series compensated transmission Test Network

The proposed fault events ascertaining scheme is validated on the 400 kV, 50 Hz, mid-point capacitor compensated simulated test network (already described in chapter 3) for

various fault scenarios. The schematic diagram of the simulated test network is shown in Figure 4.3. This EMD based scheme is also tested for all sorts of shunt fault events, and evolving fault events with different varying conditions. The 3-phase post fault current samples retrieved from the sending side are fragmented into different frequency components using EMD mechanism. Figure 4.4 shows the 3-phase post fault current samples retrieved during AG fault event at 30 km in the test network from the sending side on different inception angles. The EMD based segmentation of the post fault current sample of phase 'A' is demonstrated in Figure 4.5. Thereafter, the FFT of the obtained IMFs are computed for identifying the desirable IMFs coefficient. Figure 4.6 represents the plots of FFT analysis applied on the five different IMFs obtained after the decomposing the phase 'A' fault current signal using EMD. By analysing the FFT response, the IMFs-2 has been selected as the desired IMFs for acquiring the fault feature vectors as it has the dominant similar frequency band. Then, the fault feature vectors are extracted in terms of the energy level of the selected IMFs coefficients for each phase (i.e. Ea, Eb, and Ec). Later on the computed feature vectors corresponding to different abnormality scenarios are utilized as the training and testing dataset in the non-parametric ML classifiers models. During testing, the classifier models compute the distance of the test dataset with the pre-learned training pattern set and on that basis it predicts the class label of the test instance. The fault events classification accuracy percentage has been estimated by expression given below-

$$Classfication_{accuracy}\left(\%\right)=\frac{\left(\text{Total correct classified events}\right)}{\text{Total number of test events}}\times 100 \tag{4.1}$$

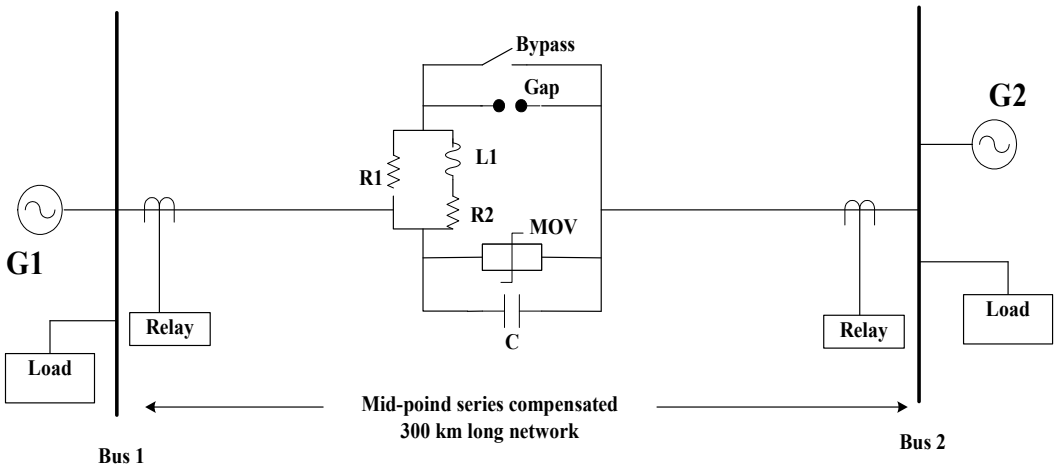

Figure 4.3 Two-bus mid-point compensated network (first test system)

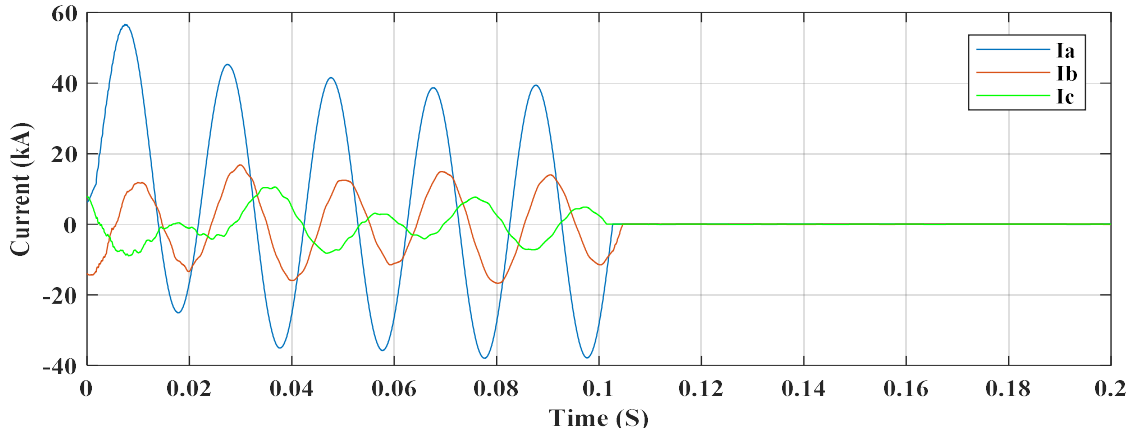

(a)

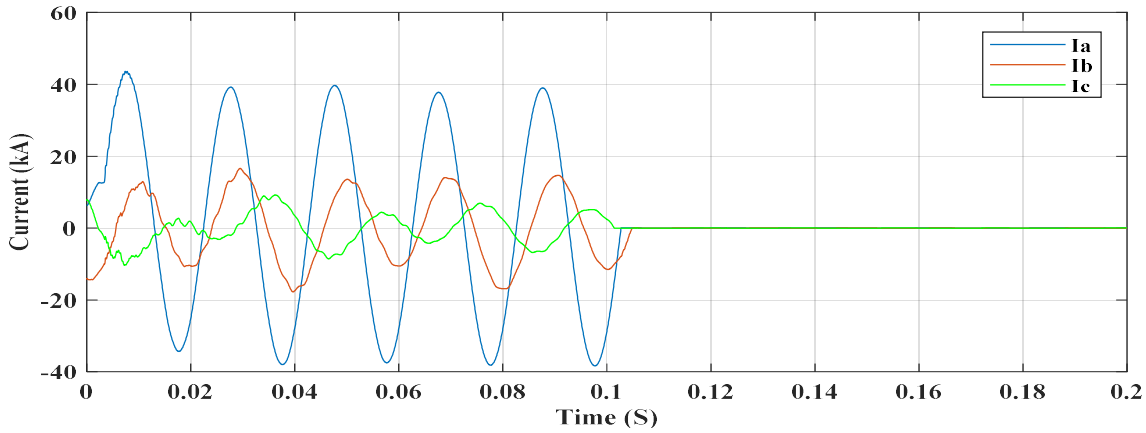

(b)

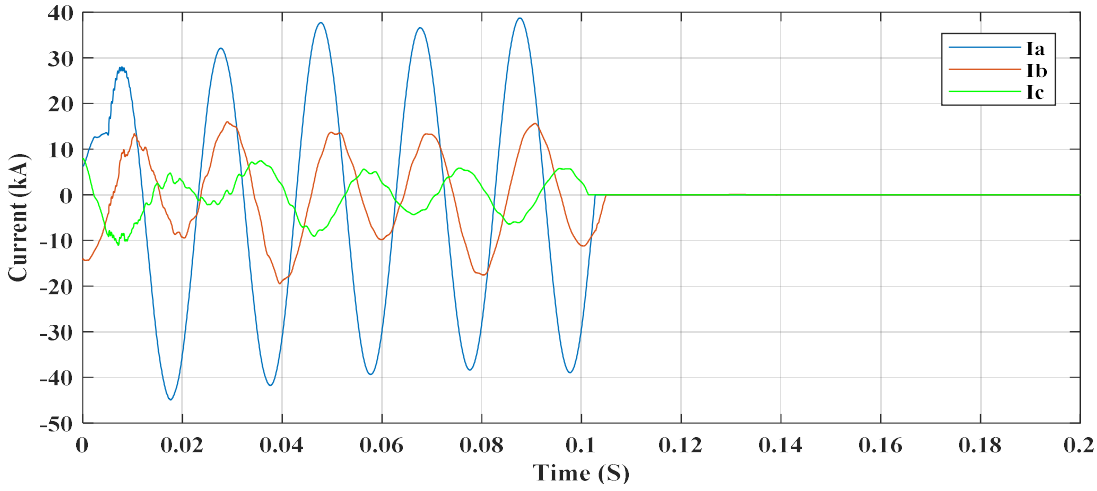

(c)

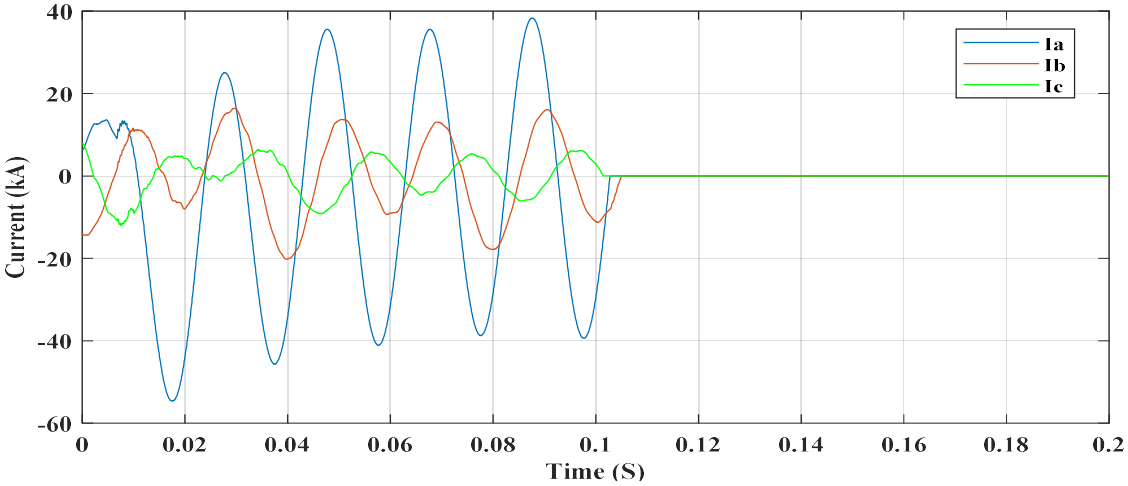

(d)

Figure 4.4 Three phase current signals during line to ground fault event at 30 km on different inception angles (a) 30 degree; (b) 60 degree; (c) 90 degree; (d) 120 degree

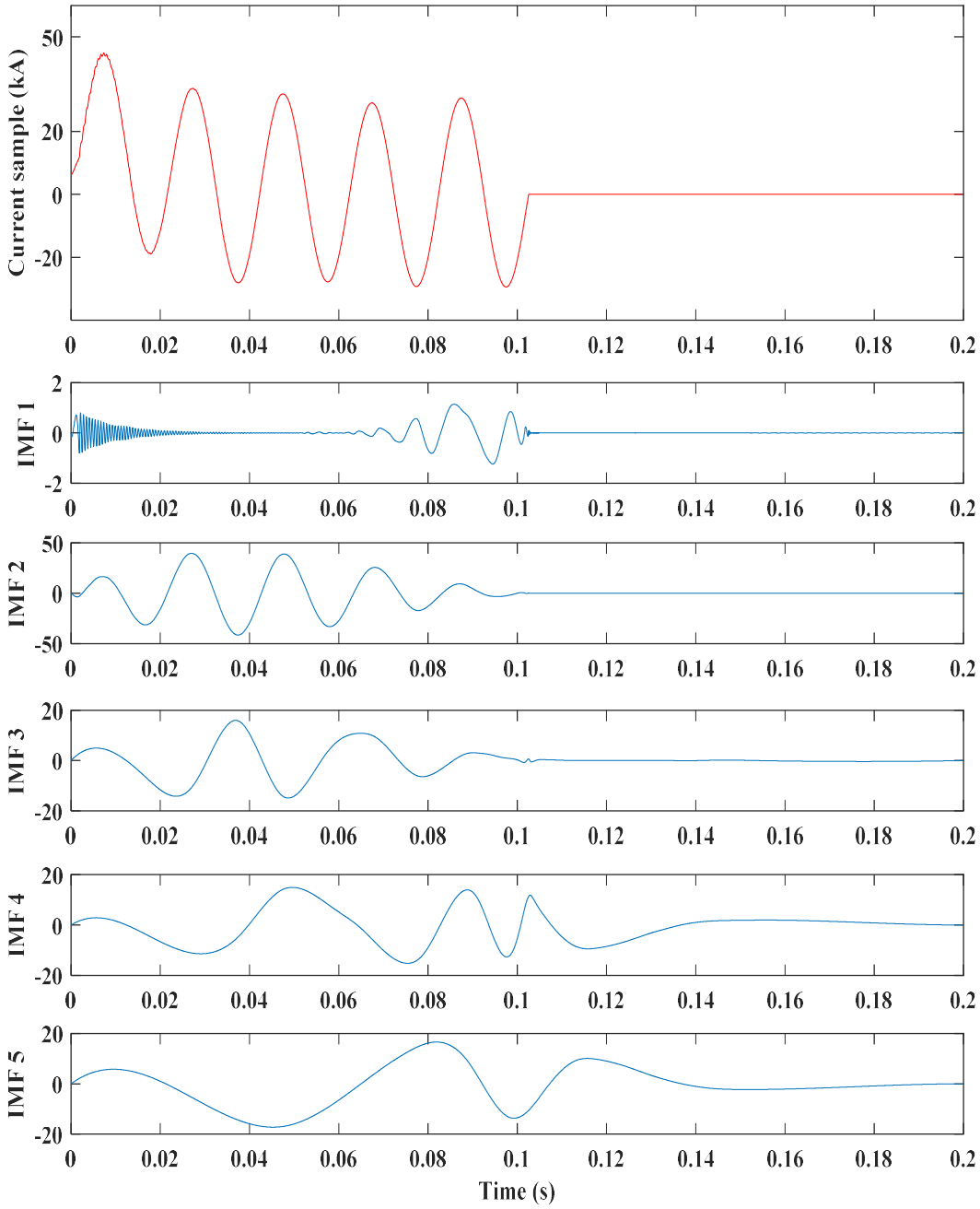

Figure 4.5 Post-fault phase 'A' current signal decomposition using EMD

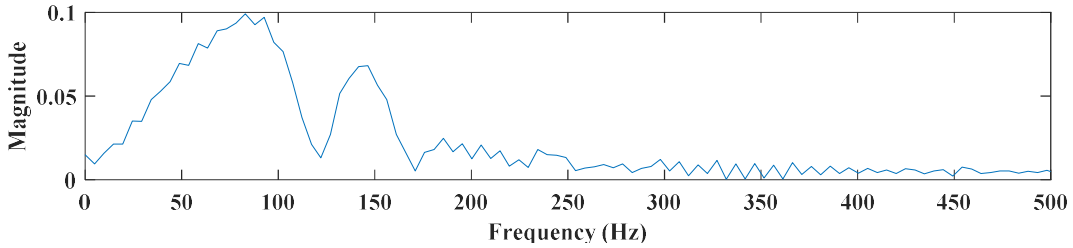

(a) IMFs-1

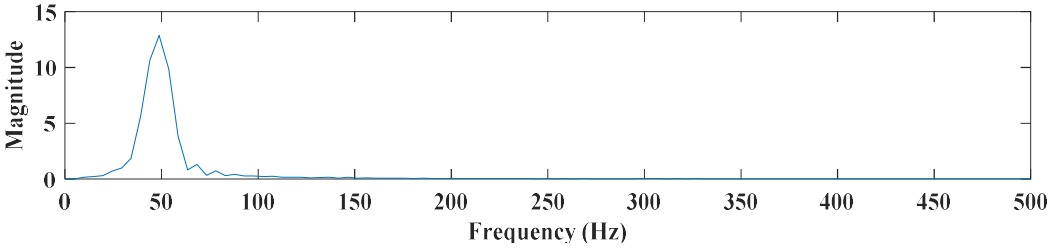

(b) IMFs-2

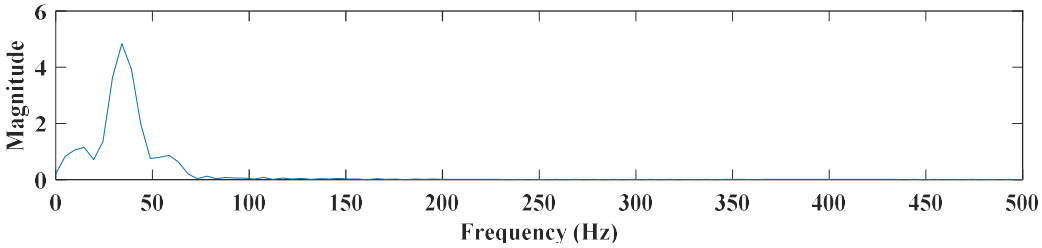

(c) IMFs-3

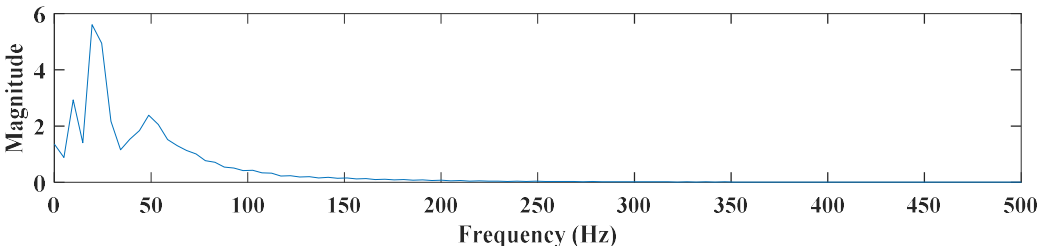

(d) IMFs-4

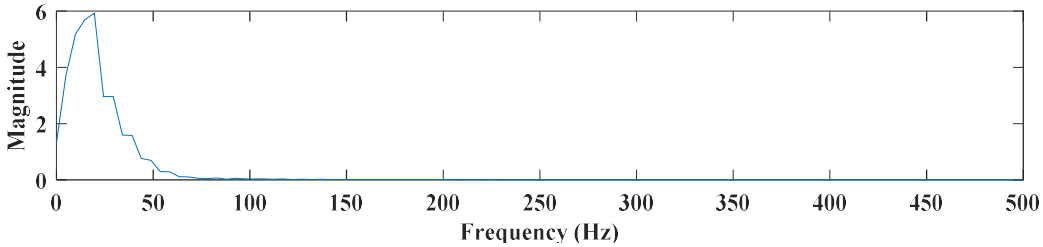

(e) IMFs-5

Figure 4.6 FFT responses of different acquired IMFs

Table 4.2 shows the fault events classification accuracy percentage obtained by the proposed EMD and K-NN based scheme during testing. As per Table 4.2, it has been observed the presented scheme gives 100 % classification accuracy for line to ground and 3-phase fault events. The overall average events classification accuracy procured by proposed scheme is 99.388 %. The corresponding confusion matrix obtained during testing of the proposed scheme is shown in Table 4.3.

Table 4.2 Faults classification accuracy percentage obtained by K-NN technique based scheme

Fault type	Number of test samples	Number of incorrect classification	Correct classification	Over all Accuracy (%)
Line to Ground	1512	0	1512	100.00
Line to Line	1512	16	1496	98.942
Double Line to Ground	1512	21	1491	98.611
3 phase (LLL)	504	0	504	100.00
Avg. Accuracy				**99.388**

Table 4.3 Confusion matrix for the KNN based scheme (First test system)

Actual fault events	Sample size	Predicted fault events											
		AG	BG	CG	AB	AC	BC	ABG	BCG	ACG	ABC	No fault	Accuracy (%)
AG	**504**	**504**	0	0	0	0	0	0	0	0	0	0	**100**
BG	**504**	0	**504**	0	0	0	0	0	0	0	0	0	**100**
CG	**504**	0	0	**504**	0	0	0	0	0	0	0	0	**100**
AB	**504**	0	0	0	**497**	0	0	**7**	0	0	0	0	**98.6**
AC	**504**	0	0	0	0	**499**	0	0	0	**5**	0	0	**99.0**
BC	**504**	0	0	0	0	0	**500**	0	**4**	0	0	0	**99.2**
ABG	**504**	0	0	0	**7**	0	0	**497**	0	0	0	0	**98.6**
BCG	**504**	0	0	0	0	0	**4**	0	**500**	0	0	0	**99.2**
ACG	**504**	0	0	0	0	**10**	0	0	0	**494**	0	0	**98.0**
ABC	**504**	0	0	0	0	0	0	0	0	0	**504**	0	**100**
No fault	**10**	0	0	0	0	0	0	0	0	0	0	**10**	**100**

Table 4.4 provides the fault events classification accuracy percentage obtained by the proposed EMD and SVM based scheme during testing. The overall average fault events classification accuracy obtained by the proposed EMD based scheme is 99.39%. Table 4.5 shows the corresponding confusion matrix obtained during the testing.

Table 4.4 Faults classification accuracy percentage obtained by SVM technique based scheme

Fault type	Number of test samples	Number of incorrect classification	Correct classification	Over all Accuracy (%)
Line to Ground	1512	0	1512	100.00
Line to Line	1512	22	1490	98.54
Double Line to Ground	1512	18	1494	98.80
3 phase (LLL)	504	0	504	100.00
Avg. Accuracy				99.34

Table 4.5 Confusion matrix for the SVM based scheme (First test system)

Actual fault events	Sample size	Predicted fault events											
		AG	BG	CG	AB	AC	BC	ABG	BCG	ACG	ABC	No fault	Accuracy (%)
AG	**504**	**504**	0	0	0	0	0	0	0	0	0	0	**100**
BG	**504**	0	**504**	0	0	0	0	0	0	0	0	0	**100**
CG	**504**	0	0	**504**	0	0	0	0	0	0	0	0	**100**
AB	**504**	0	0	0	**491**	0	0	**13**	0	0	0	0	**97.4**
AC	**504**	0	0	0	0	**498**	0	0	0	**6**	0	0	**98.8**
BC	**504**	0	0	0	0	0	**501**	0	**3**	0	0	0	**99.4**
ABG	**504**	0	0	0	**6**	0	0	**498**	0	0	0	0	**98.8**
BCG	**504**	0	0	0	0	0	**4**	0	**500**	0	0	0	**99.2**
ACG	**504**	0	0	0	0	**8**	0	0	0	**496**	0	0	**98.4**
ABC	**504**	0	0	0	0	0	0	0	0	0	**504**	0	**100**
No fault	**10**	0	0	0	0	0	0	0	0	0	0	**10**	**100**

Table 4.6 presents the fault events classification accuracy percentage obtained by the proposed EMD and PNN based scheme during testing. It has been observed that the EMD and PNN based scheme gives 100%, 99.53%, 99.0%, and 100% events classification accuracy for LG, LL, LLG and LLL fault events respectively. By seeing the results procured after the validation of proposed scheme on first test network, it have been reasserted that the proposed EMD and ML based approach is well efficient and precise in identifying the particular class of the faults with very good accuracy. Figure 4.7 shows the associated PNN confusion matrix.

Table 4.6 Faults classification accuracy percentage obtained by PNN technique based scheme

Fault type	Number of test samples	Number of incorrect classification	Correct classification	Over all Accuracy (%)
Line to Ground	1512	0	1512	100.00
Line to Line	1512	9	1503	99.40
Double Line to Ground	1512	17	1495	98.88
3 phase (LLL)	504	0	504	100.00
Avg. Accuracy				**99.57**

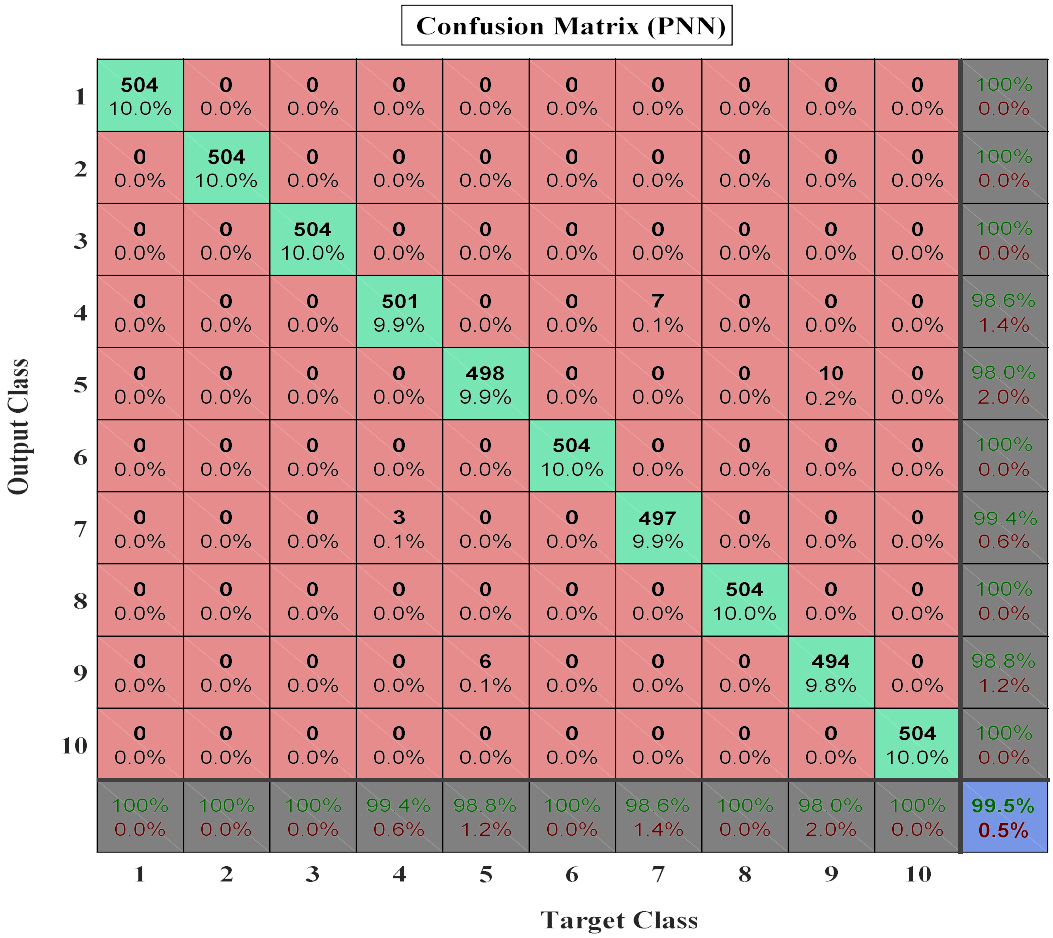

Figure 4.7 Confusion matrix during events classification using PNN classifier model

Table 4.7 provides the details of the time response taken by the different ML classifier based approaches for predicting the categories of fault events in the network. Table 4.8 represents the comparative result in terms of average events classification accuracy procured by the proposed EMD and ML based schemes with some already available approaches in the literature [58, 39, 32, and 40]. As seen from the Table 4.8, the proposed scheme gives better classification accuracy than that of reported by other approaches in the literature.

Table 4.7 Time of response of different non-parametric ML scheme

S. No	Non-Parametric ML Classifier Model Utilized	Time of response
i	K-NN	3.875e-02 s
ii.	SVM	2.190e-02 s
iii.	PNN	1.46e-01 s

Table 4.8 Comparative study of average classification accuracy achieved by the proposed scheme with previously reported protection approaches

Fault type	Ref. [58] (%)	Ref. [39] (%)	Ref. [32] (%)	Ref. [40] (%)	(SVM) (%)	(KNN) (%)	(PNN) (%)
Line to ground	97.23	97.447	100.00	99.449	100.00	100.00	100.00
Line to line	97.29	99.616	97.560	97.687	98.54	98.942	99.40
Double line to ground	97.84	98.611	98.788	99.314	98.80	98.611	98.88
3 phase (LLL)	97.68	100.00	100.00	98.565	100.00	100.00	100.00
Average accuracy	**97.51**	**98.918**	**99.087**	**98.753**	**99.34**	**99.388**	**99.57**

4.3.2 Test case II: Modified IEEE 9-Bus Series Compensated Test Network

The competency of the proposed EMD and ML based events categorization scheme is also evaluated on the second simulated modified 9-bus test network (shown in Figure 4.8). All

kinds of shunt fault events and evolving fault events have been considered during the testing of second test network. The details of different simulated training and testing conditions on second test network are listed in Table 3.10. Figure 4.9 shows the 3-phase post fault (A-G) current signal measured at 50 km from the sending side on different inception angles. The retrieved post fault current samples are decomposed into five IMFs using EMD mechanism. Figure 4.9 represents the decomposed version of the post fault current signal of phase 'A' into five distinct IMFs. Subsequently, the FFT mechanism has been applied on the obtained IMFs for identifying the desired IMFs which has the similar frequency range. Figure 4.11 represents the plots of FFT analysis applied on the obtained IMFs. By observing the FFT responses (shown in Figure 4.11) the IMFs-2 has been shortlisted as the needed IMFs for extracting the fault feature vectors. Afterwards, the fault features are extracted in terms of the energy level of the selected IMFs coefficients for each phase (i.e. Ea, Eb, and Ec). Later on the extracted feature vectors corresponding to different fault scenarios in the transmission circuit are utilized as the training and testing dataset in the non-parametric ML classifiers models. In the testing phase, the classifier models compute the distance of the test instance from the pre learned training pattern set and on that basis the model predicts the particular class label of the test case as its output.

Table 4.9 Training and testing conditions considered on second test system

S. No	Parameters	Training cases	Testing cases
1.	Fault locations	Twenty different locations	Five new unknown location (50 km, 110 km, 170 km, 210 km and 250 km)
2.	Fault Resistance (ohms)	0.001, 15, 30	0.1, 1, 5, and 10
3.	Fault inception angle (degree)	0, 75, 150	30, 45, 60, 90, and 120
4.	Fault events types	No fault and all kinds faults events	Normal operation mode and all kinds of fault events (unfamiliar)
5.	Level of line compensation	35 % and 45 %	30 % and 40 %

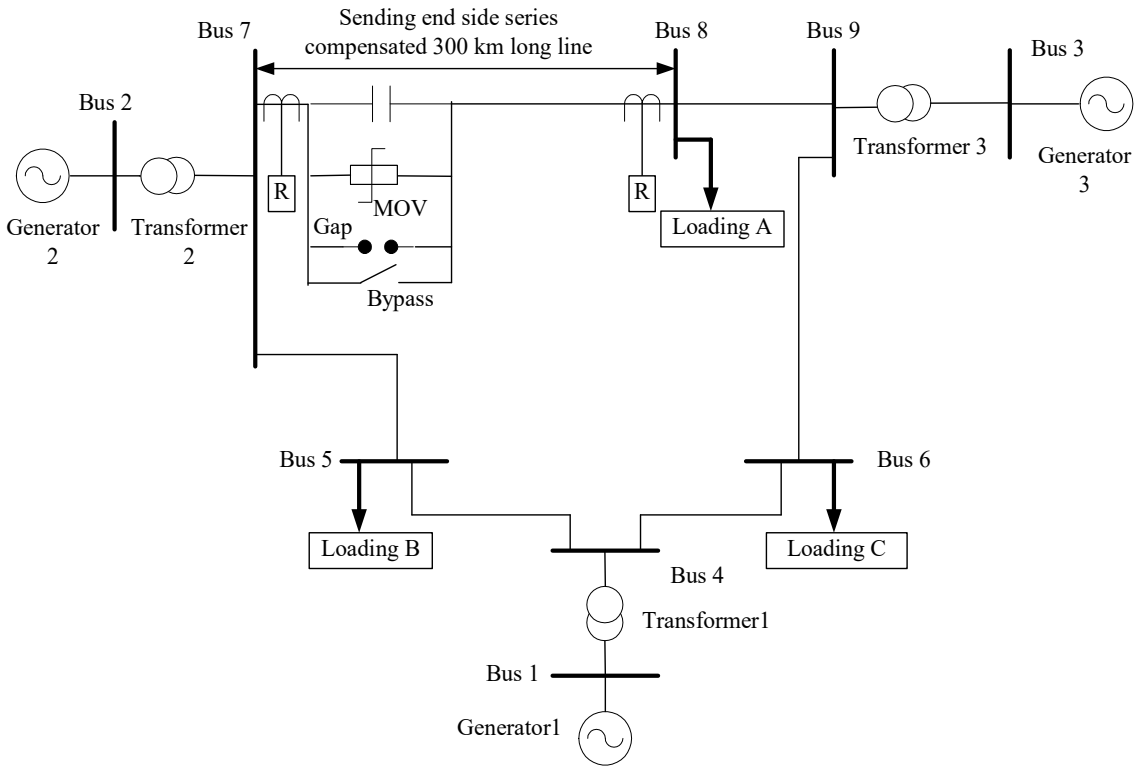

Figure 4.8 Simulated modified WSCC 9-Bus IEEE network (second test system)

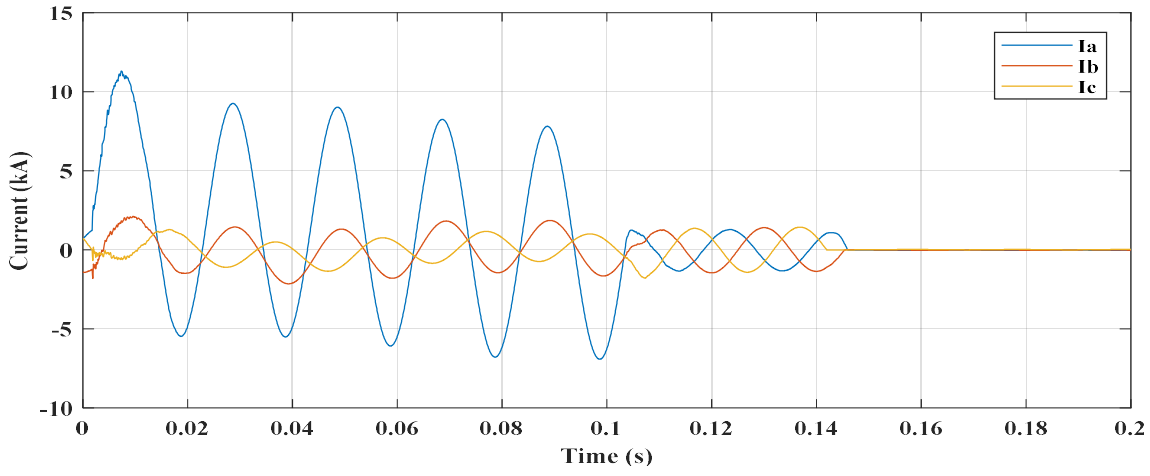

(a)

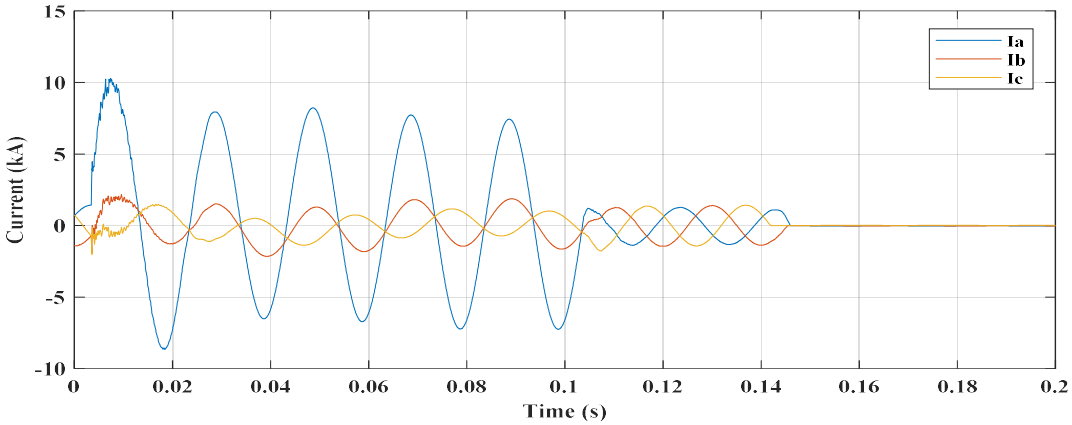

(b)

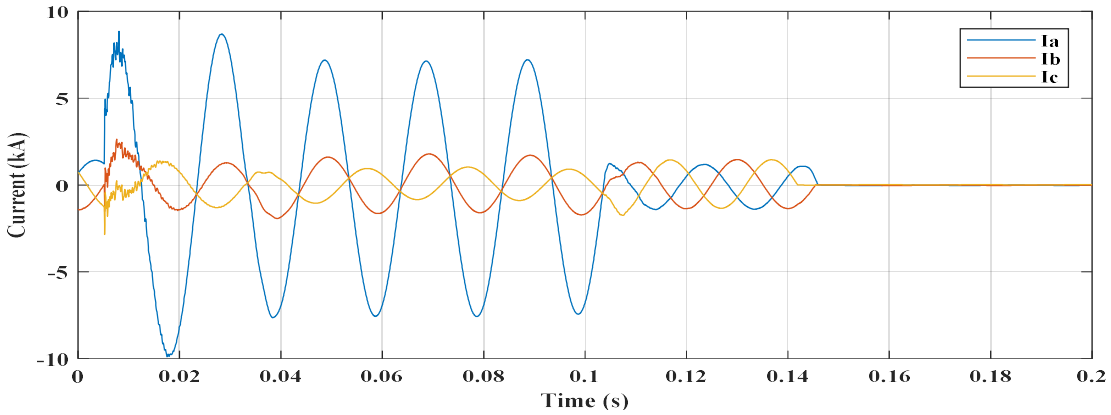

(c)

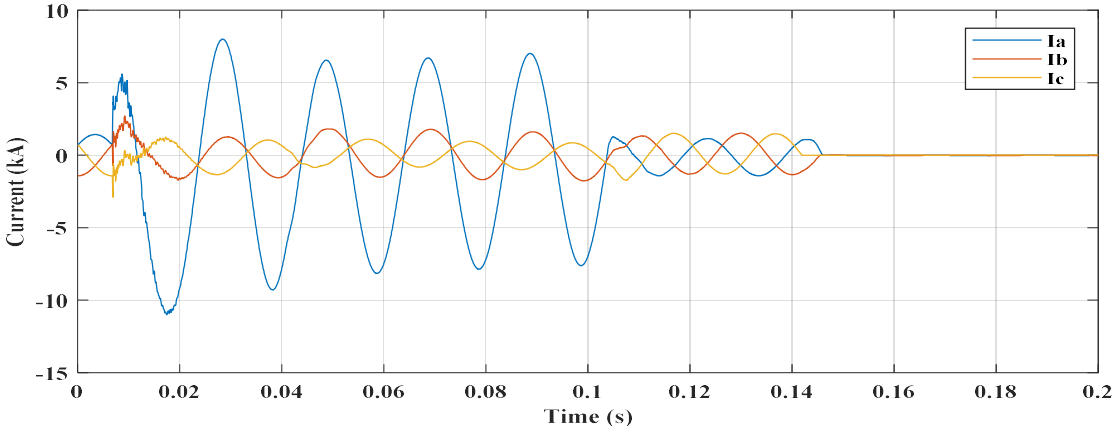

(d)

Figure 4.9 Three phase current signals during line to ground fault event at 50 km on different inception angles (a) 30 degree; (b) 60 degree; (c) 90 degree; (d) 120 degree

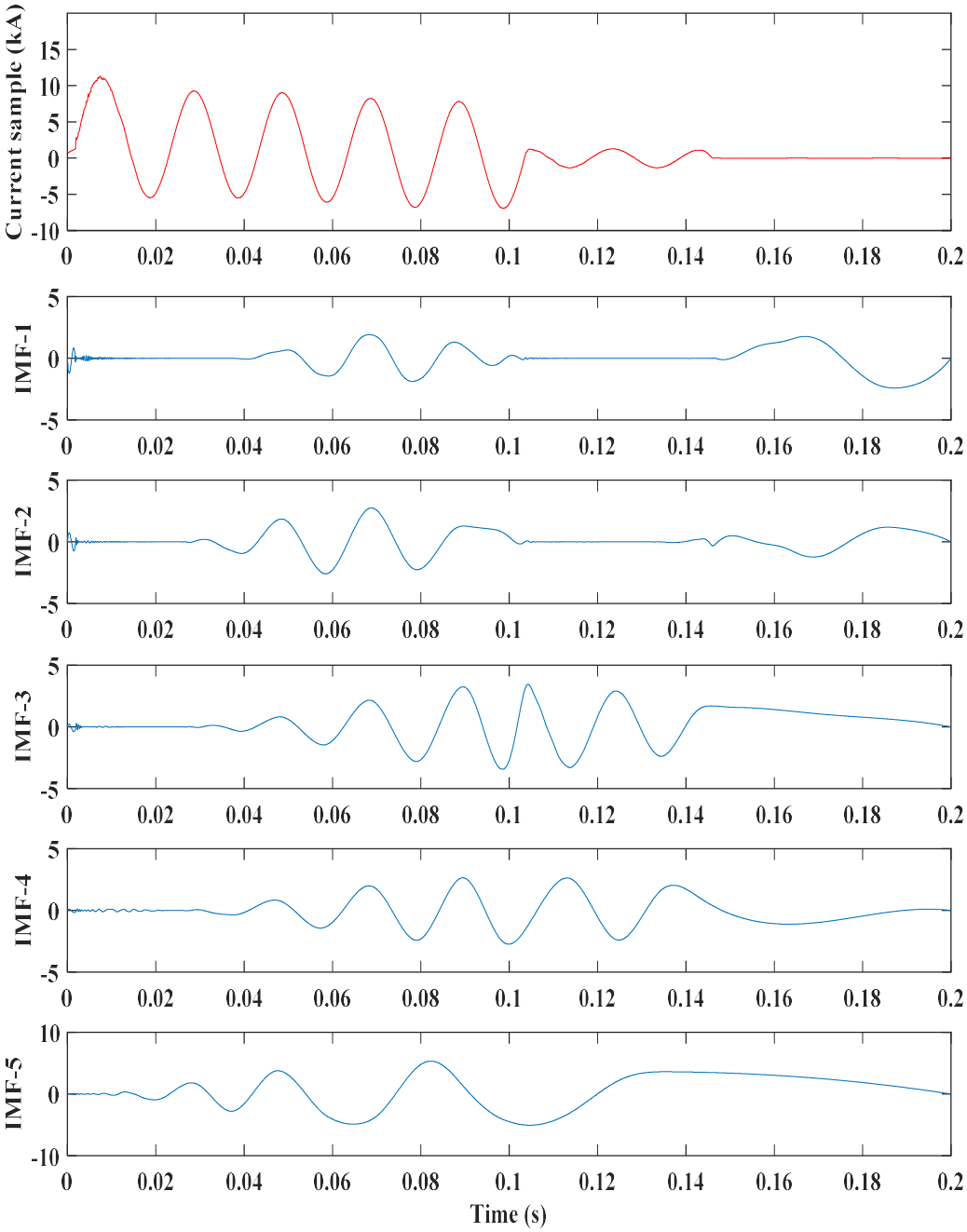

Figure 4.10 Post-fault phase 'A' current signal decomposition using EMD

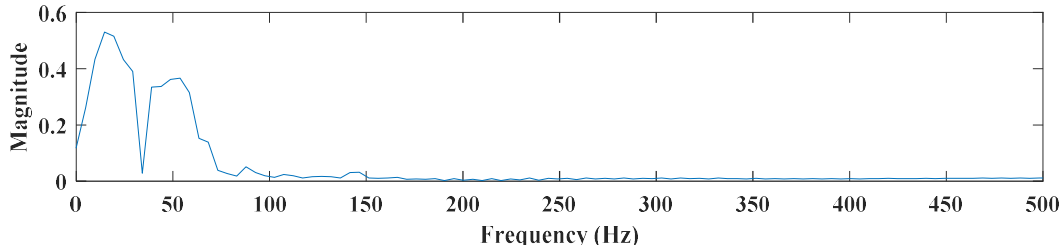

(a) IMFs-1

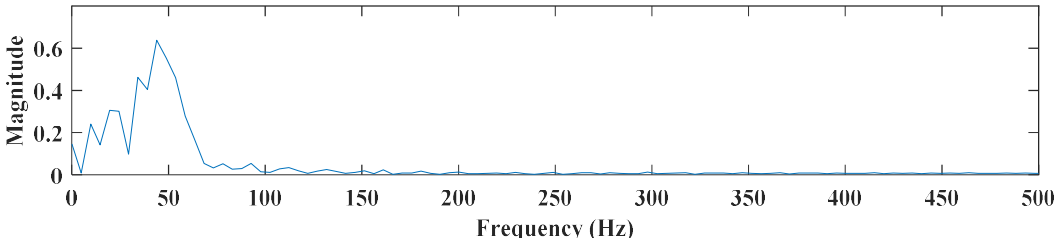

(b) IMFs-2

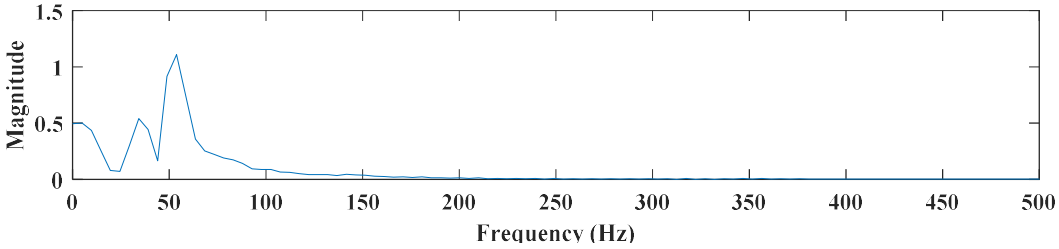

(c) IMFs-3

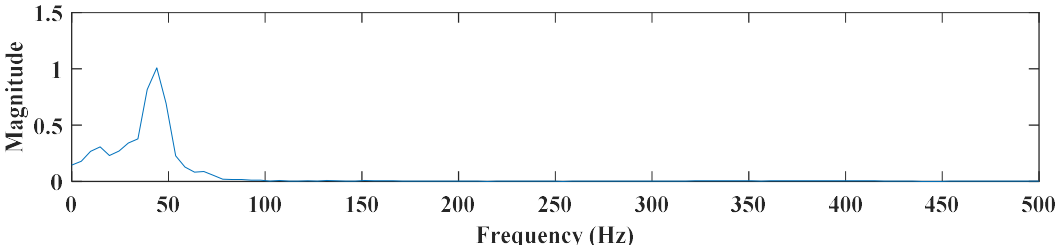

(d) IMFs-4

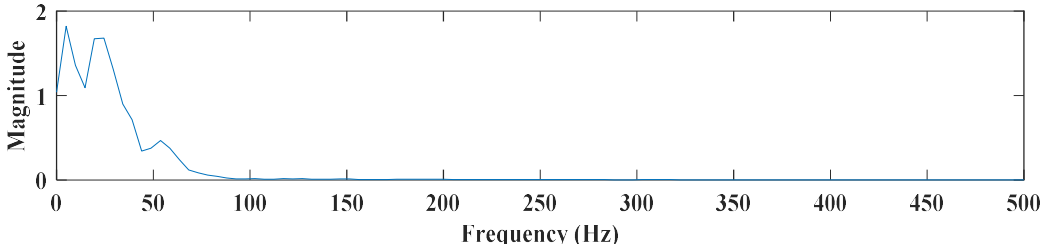

(e) IMFs-5

Figure 4.11 FFT responses of different acquired IMFs

The fault events classification accuracy procured by the proposed EMD and K-NN based approach during testing on the second test network are depicted in Table 4.10. From Table 4.10, it can be seen that proposed K-NN based scheme gives 99.24% overall average classification accuracy for various considered test cases in the second test network. Table 4.11 presents the corresponding confusion matrix during testing for KNN based approach.

Table 4.10 Faults classification accuracy percentage obtained by K-NN technique based scheme

Fault type	Number of test samples	Number of incorrect classification	Correct classification	Over all Accuracy (%)
Line to Ground	600	0	600	100.00
Line to Line	600	7	593	98.83
Double Line to Ground	600	11	589	98.16
3 phase (LLL)	200	0	200	100.00
Avg. Accuracy				**99.24**

Table 4.11 Confusion matrix for KNN based scheme (second test system)

Actual fault events	Sample size	Predicted fault events											
		AG	BG	CG	AB	AC	BC	ABG	BCG	ACG	ABC	No fault	Accuracy (%)
AG	**200**	**200**	0	0	0	0	0	0	0	0	0	0	**100**
BG	**200**	0	**200**	0	0	0	0	0	0	0	0	0	**100**
CG	**200**	0	0	**200**	0	0	0	0	0	0	0	0	**100**
AB	**200**	0	0	0	**197**	0	0	**3**	0	0	0	0	**98.5**
AC	**200**	0	0	0	0	**194**	0	0	0	**4**	0	0	**97.0**

BC	**200**	0	0	0	0	0	**200**	0	0	0	0	0	**100**
ABG	**200**	0	0	0	**4**	0	0	**196**	0	0	0	0	**98.0**
BCG	**200**	0	0	0	0	0	**2**	0	**198**	0	0	0	**99.0**
ACG	**200**	0	0	0	0	**5**	0	0	0	**195**	0	0	**97.5**
ABC	**200**	0	0	0	0	0	0	0	0	0	**200**	0	**100**
No fault	**10**	0	0	0	0	0	0	0	0	0	0	**10**	**100**

Table 4.12 Faults classification accuracy percentage obtained by SVM technique based scheme

Fault type	Number of test samples	Number of incorrect classification	Correct classification	Over all Accuracy (%)
Line to Ground	600	0	600	100.00
Line to Line	600	14	586	97.67
Double Line to Ground	600	9	591	98.50
3 phase (LLL)	200	0	200	100.00
Avg. Accuracy				**99.04**

Table 4.12 presents the fault events classification accuracy obtained by the proposed EMD and SVM based approach during testing on second test system. As seen from the table, the overall average fault events classification accuracy acquired by SVM based classifier model is 99.04%. The associated confusion matrix for SVM based approach is shown in Table 4.13.

Table 4.13 Confusion matrix for SVM based scheme (Second test system)

Actual fault events	Sample size	Predicted fault events											
		AG	BG	CG	AB	AC	BC	ABG	BCG	ACG	ABC	No fault	Accuracy (%)
AG	**200**	**200**	0	0	0	0	0	0	0	0	0	0	**100**
BG	**200**	0	**200**	0	0	0	0	0	0	0	0	0	**100**
CG	**200**	0	0	**200**	0	0	0	0	0	0	0	0	**100**
AB	**200**	0	0	0	**192**	0	0	**8**	0	0	0	0	**96.0**
AC	**200**	0	0	0	0	**196**	0	0	0	**4**	0	0	**98.0**
BC	**200**	0	0	0	0	0	**198**	0	**2**	0	0	0	**99.0**
ABG	**200**	0	0	0	**4**	0	0	**196**	0	0	0	0	**98.0**
BCG	**200**	0	0	0	0	0	0	0	**200**	0	0	0	**100**
ACG	**200**	0	0	0	0	**5**	0	0	0	**194**	0	0	**97.0**
ABC	**200**	0	0	0	0	0	0	0	0	0	**200**	0	**100**
No fault	**10**	0	0	0	0	0	0	0	0	0	0	**10**	**100**

Table 4.14 Faults classification accuracy percentage obtained by PNN technique based scheme

Fault type	Number of test samples	Number of incorrect classification	Correct classification	Over all Accuracy (%)
Line to Ground	600	0	600	100.00
Line to Line	600	0	600	100.00
Double Line to Ground	600	6	594	99.00
3 phase (LLL)	200	0	200	100.00
Avg. Accuracy				99.75

Table 4.14 presents the fault events classification accuracy obtained by the proposed EMD and PNN based approach during testing on second test network. The overall average accuracy observed by the applying the PNN technique based classifier model is 99.75%. The Figure 4.12 shows the associated confusion matrix.

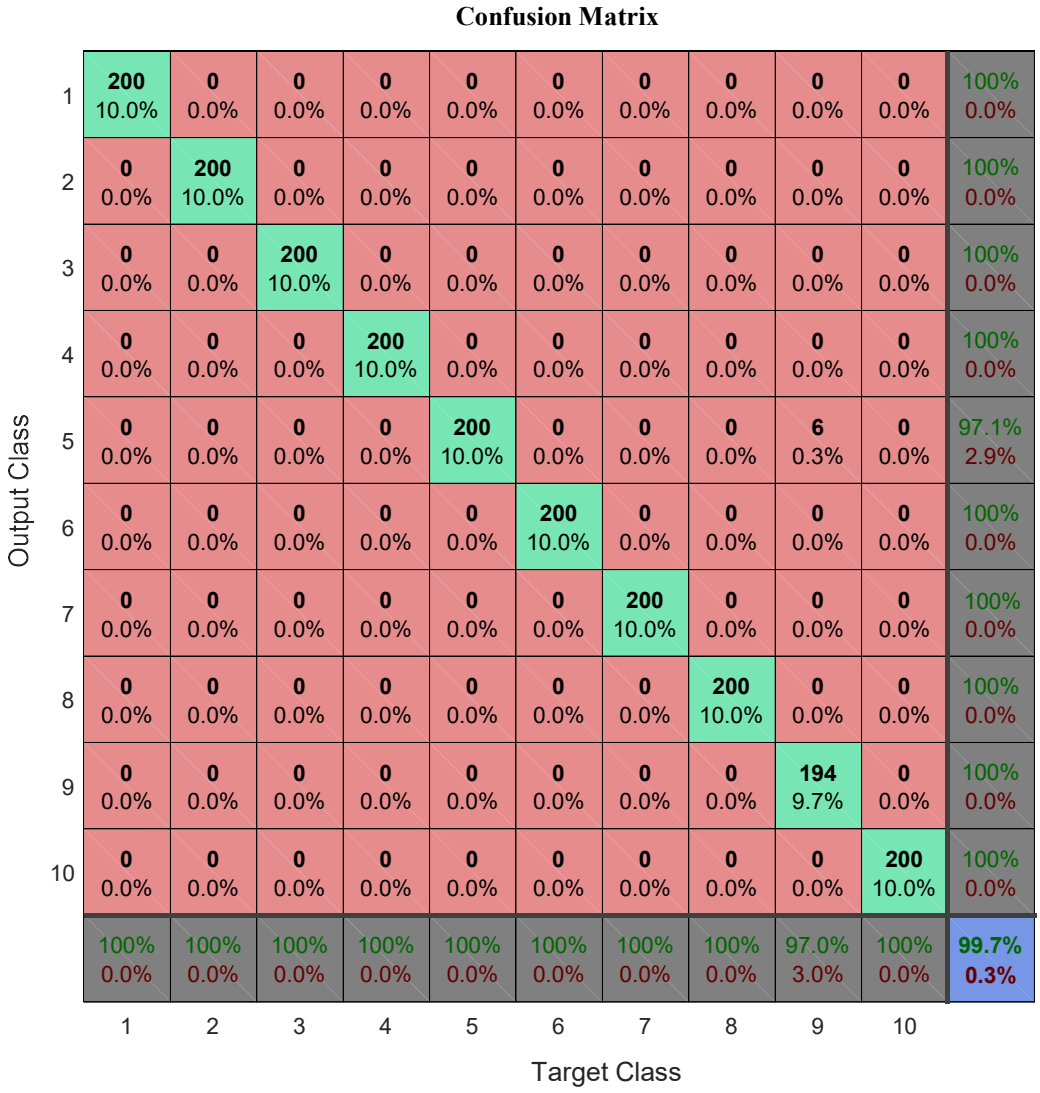

Figure 4. 12 Confusion matrix during events classification using PNN classifier model

4.4 Evolving Fault Events Identification

Evolving fault events in the power transmission circuits are usually uncommon, but these are more problematic than normal shunt fault events. These events are also called as transforming fault events as involves switching of fault phases within few time cycles. The identification of evolving events is more complicated than those of common shunt fault events in the transmission circuits. Figure 4.13 shows the 3-phase post fault current samples during the case of evolving event simulated in the test transmission circuit at 50 km from the bus 7. In all three considered cases, the primary faults are initiated as the phase A to ground fault at t= 0.00166 seconds and then transformed into other phases after 5ms. In present analysis, three different time span between the primary and secondary fault events have been considered. The details of different evolving cases considered as the training and testing conditions during the assessment of the proposed EMD and ML based events identification scheme are similar to that are utilized in the chapter 3 and are also enlisted in Table 4.15. The total size of the considered testing samples is 4200, including four types of normal shunt events, three types of evolving events, four different set of fault resistances, five inception angles, two level of line compensation percentage and three different time interval between the primary and secondary events). The post-fault current samples retrieved during different fault events are decomposed into IMFs coefficients by using EMD technique. Figure 4.14 and Figure 4.16 represents the EMD based decomposition of the post fault current signal of phase ‘A’ and phase ‘B’ during evolving fault AG-bg type. Afterwards, the FFT responses of the IMFs coefficients are computed for determining the appropriate IMFs which has similar frequency range. Figure 4.15 and 4.17 represents the plots of FFT responses on the five different acquired IMFs of phase ‘A’ and phase ‘B’ fault

current signal. By observing the FFT responses the IMFs-5 and IMFs-4 have been shortlisted as the needed IMFs for extracting the fault feature vectors. Thereafter, the fault features are computed for each phase in terms of energy level of the chosen IMFs coefficients. Later on, the extracted features associated with both normal shunt fault and evolving fault events are applied as input dataset to the non-parametric classifier models during training and testing. The multiple fault events as labelled as follows: Class 1 (AG), class 2 (ABG), class 3 (AB-bg), class 4 (ACG), class 5 (AG-cg), class 6 (ABC), class 7 (AG-abcg). Finally, the ML classifier model predicts the class label of the test fault instance on the basis of trained pattern set as its output.

Table 4.15 Training and testing conditions for assessing evolving fault events

S. No	Parameters	Training cases	Testing cases
1.	Fault locations (km)	Twenty different locations	Five new unknown location (50km, 110 km, 170 km, 210 km and 250 km)
2.	Fault Resistance (ohms)	0.001, 15, 30	0.1, 1, 5, and 10
3.	Fault inception angle (°)	0, 75, 150	30, 45, 60, 90, and 120
4.	Fault events types	AG, ABG, ACG, ABC, AG-bg, AG-cg and AG-abcg	AG, ABG, ACG, ABC, AG-bg, AG-cg and AG-abcg
5.	Level of line compensation	35 % and 45 %	30 % and 40 %
6.	Time interval span	5ms	5, 10, and 15 ms

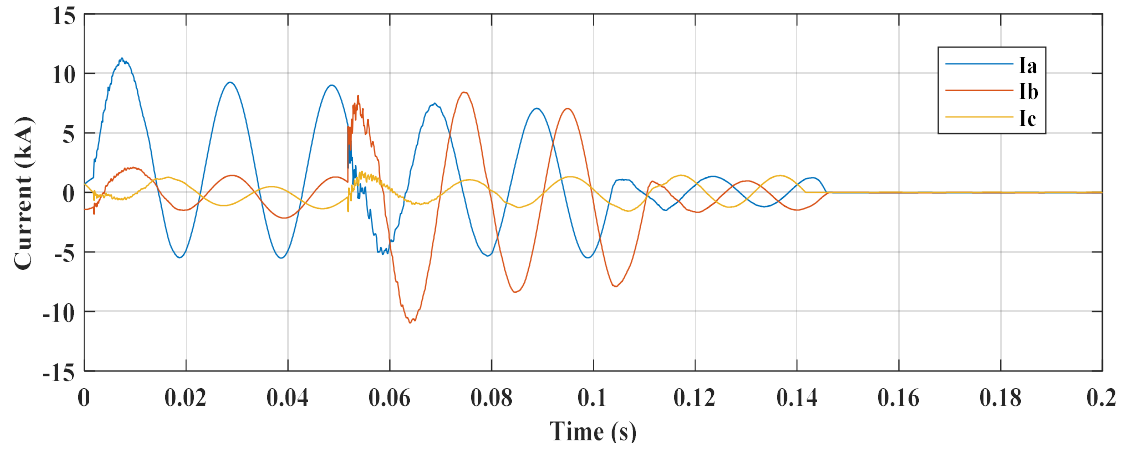

(a)

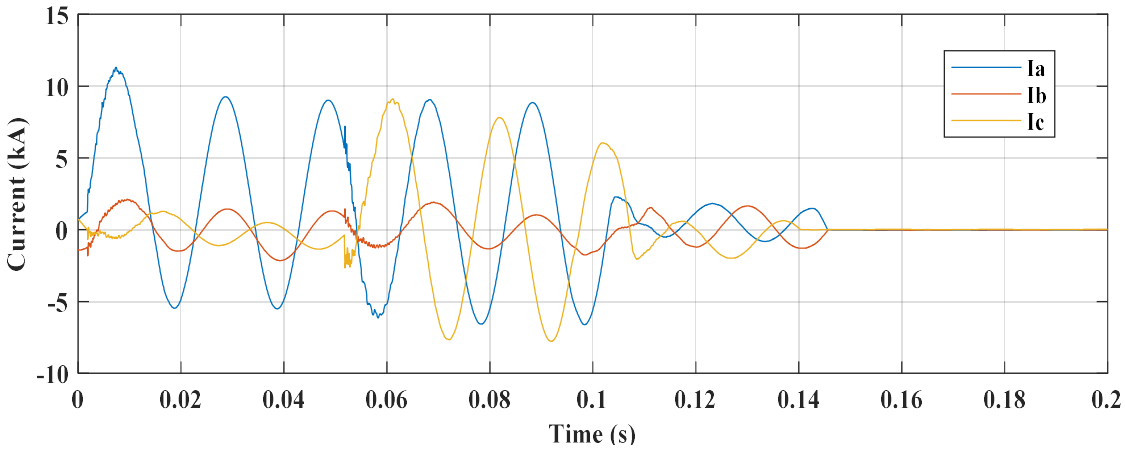

(b)

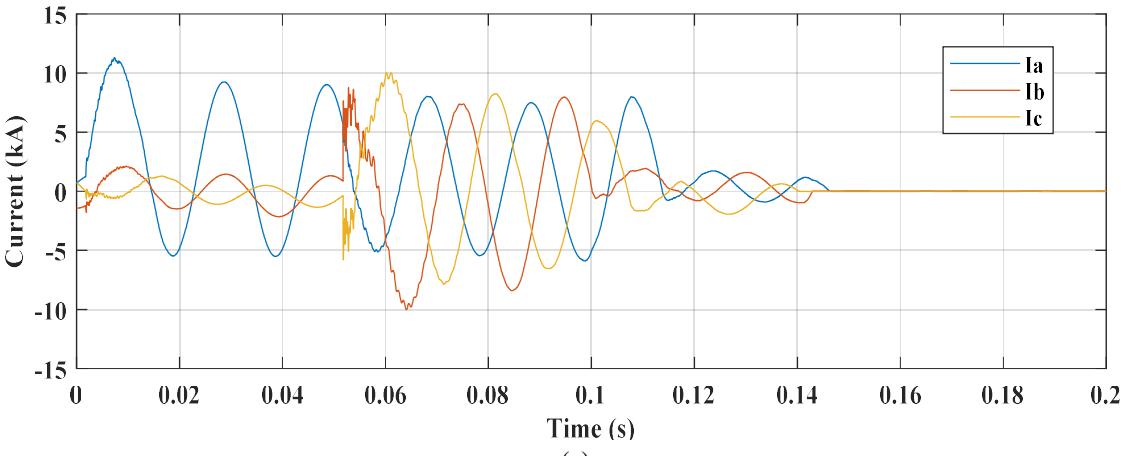

(c)

Figure: 4.13 Three-phase current samples during evolving fault in the test network (a) AG-bg at 50 km, (b) AG-cg at 50 km, (c) AG-abcg at 50 km

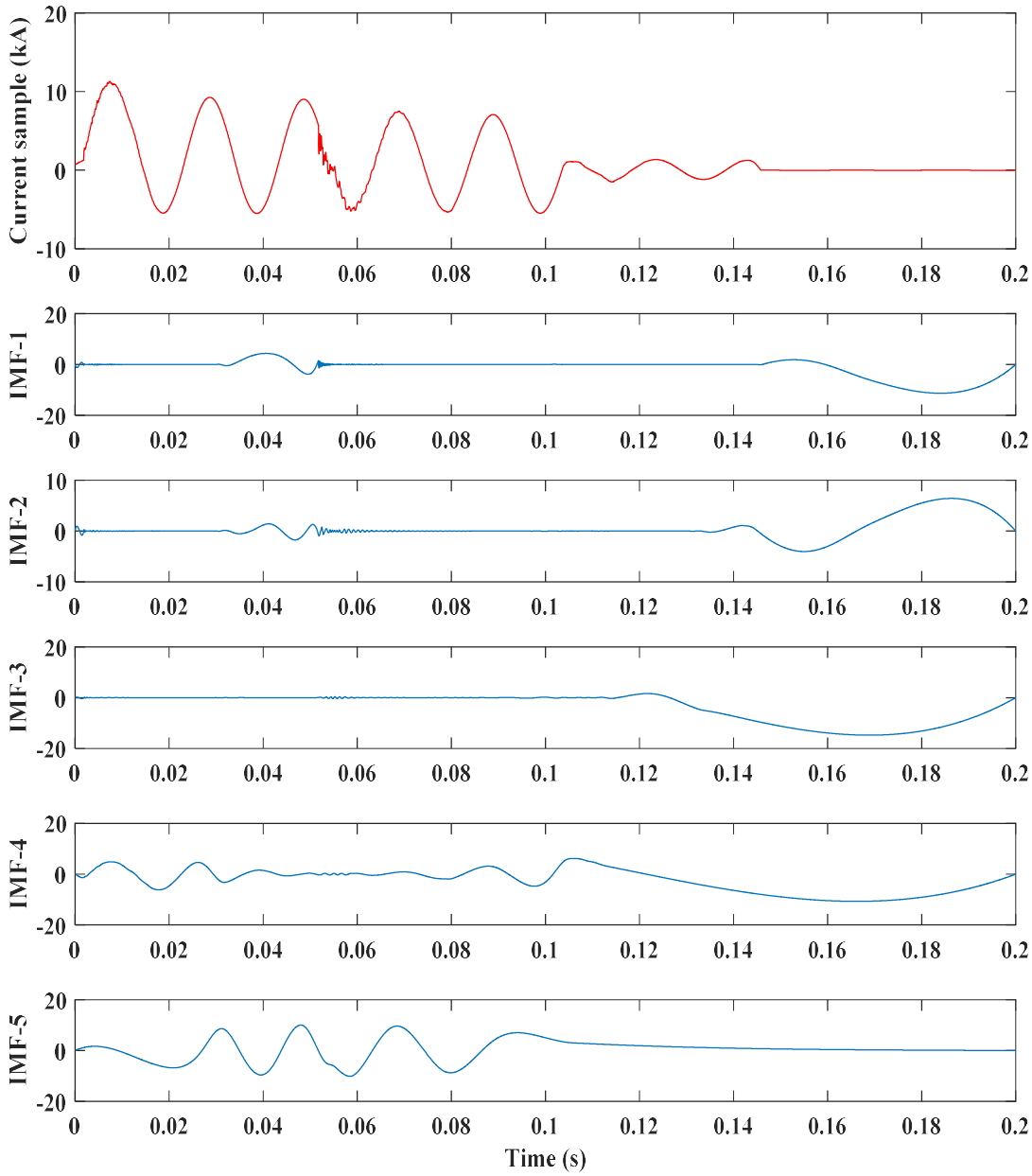

Figure 4.14 Evolving fault (phase 'A') current signal decomposition using EMD

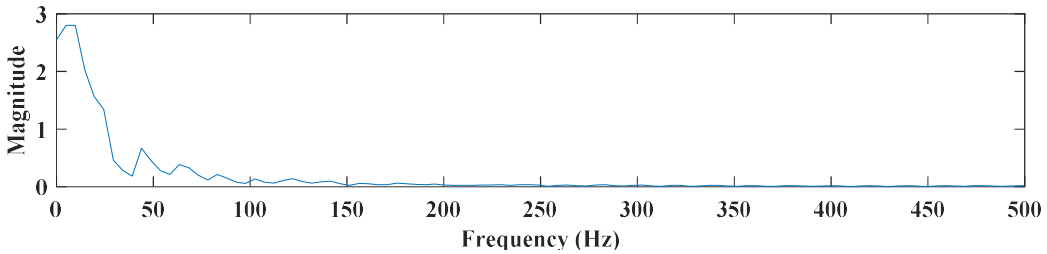

(a) IMFs-1

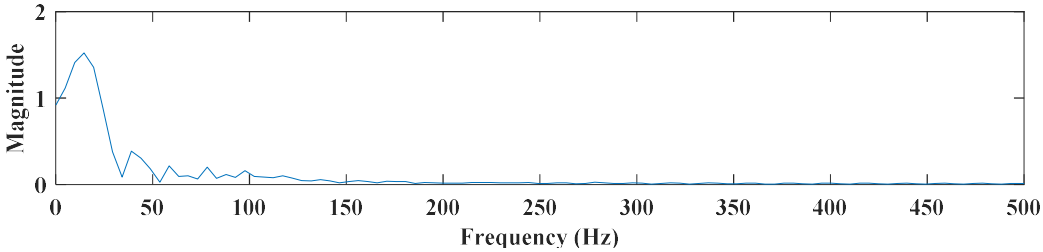

(b) IMFs-2

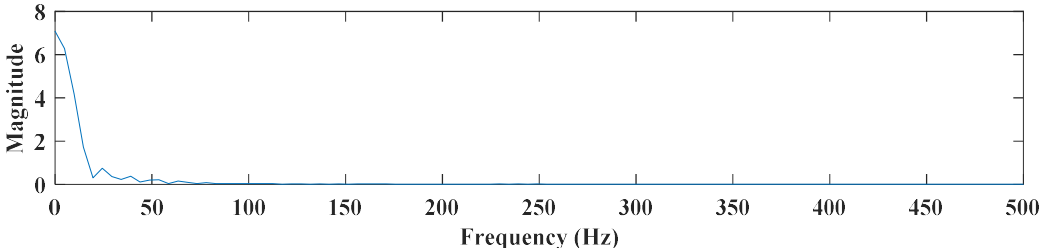

(c) IMFs-3

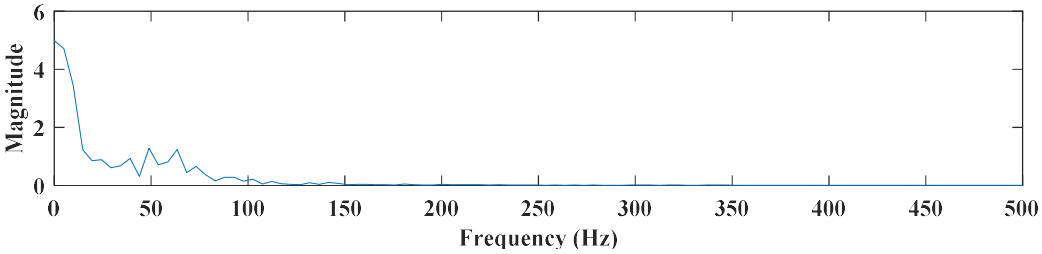

(d) IMFs-4

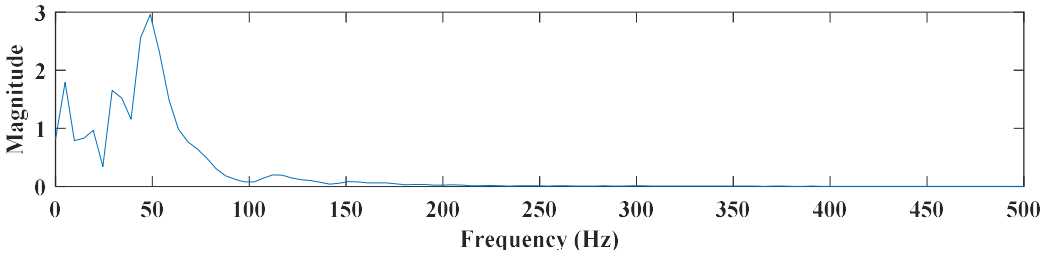

(e) IMFs-5

Figure 4.15 FFT responses of different acquired IMFs for phase ‘A’

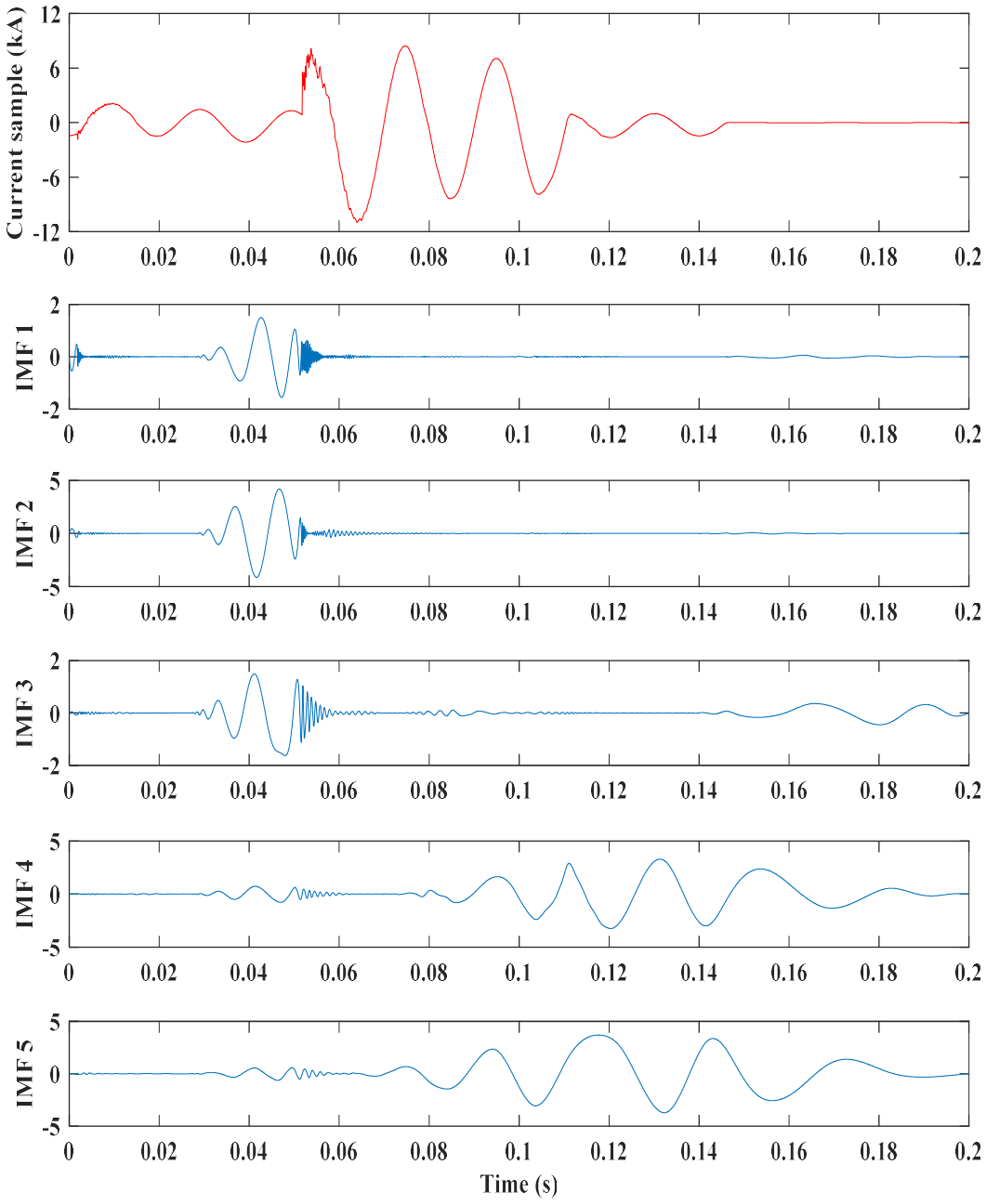

Figure 4.16 Evolving fault (phase 'B') current signal decomposition using EMD

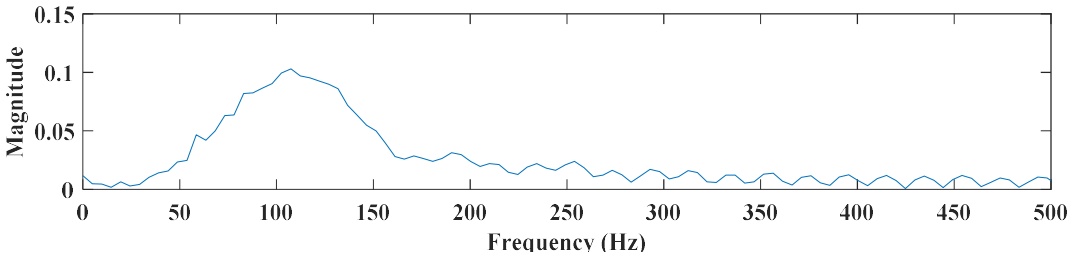

(a) IMFs-1

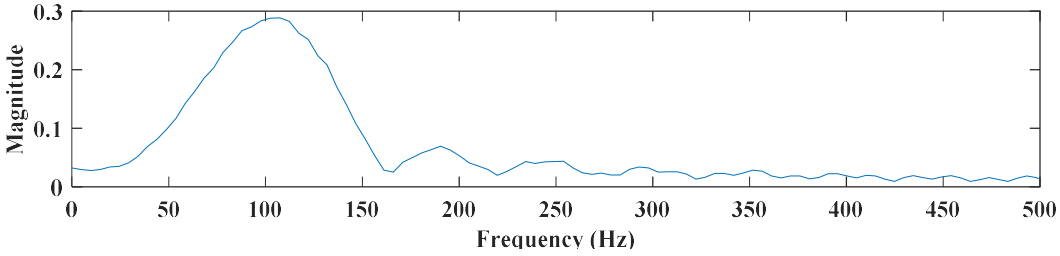

(b) IMFs-2

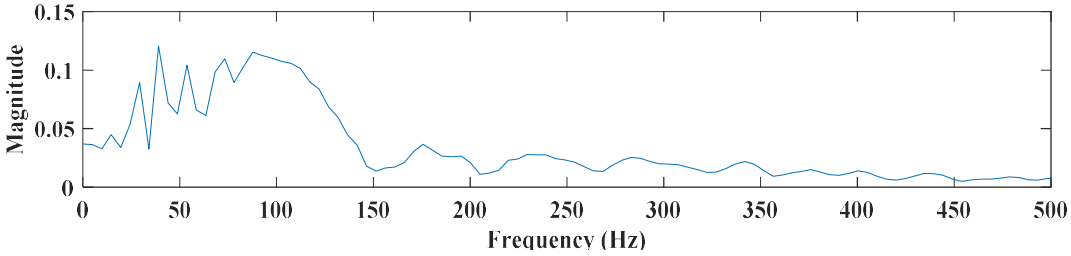

(c) IMFs-3

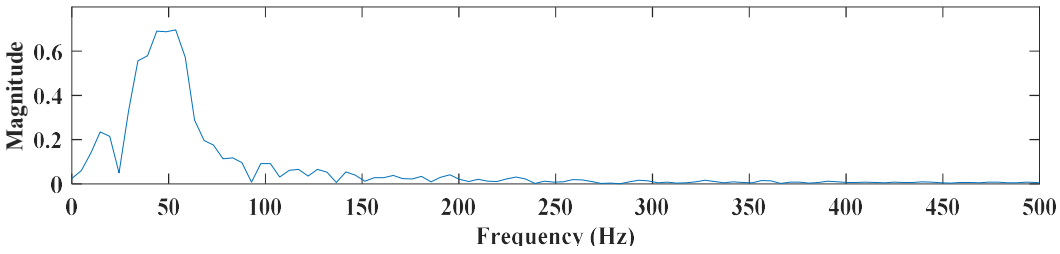

(d) IMFs-4

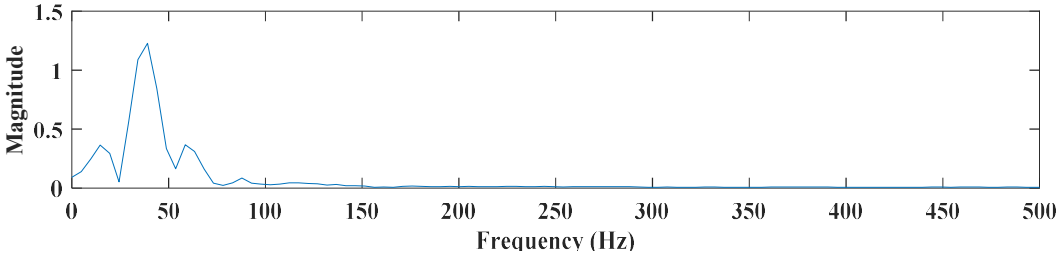

(e) IMFs-5

Figure 4.17 FFT responses of different acquired IMFs for phase 'B'

Table 4.16 shows the evolving faults classification results obtained by the proposed EMD and K-NN based scheme. Similarly, Table 4.17 represents the evolving faults classification results obtained by the proposed DWT and SVM based events ascertaining scheme. From the depicted results, it can be deduced that proposed EMD and ML based scheme is well effectual in discriminating the normal shunt faults and evolving fault events.

Table 4.16 Identification of evolving fault events using KNN classifier based scheme

S.No	Primary fault type	Secondary fault type	Time interval (ms)	Evolving Fault or not	Classifier output
1.	AG	-	-	No	1
2.	ABG	-	-	No	2
3.	AG	bg	5	Yes	3
4.	ACG	-	-	No	4
5.	AG	cg	5	Yes	5
6.	ABC	-	-	No	6
7.	AG	abcg	5	Yes	7
8.	AG	bg	10	Yes	3
9.	AG	cg	10	Yes	5
10.	AG	abcg	10	Yes	7
11.	AG	bg	15	Yes	3
12.	AG	cg	15	Yes	5
13.	AG	abcg	15	Yes	7

Table 4.17 Identification of evolving fault events using SVM classifier based scheme

S.No	Primary fault type	Secondary fault type	Time interval (ms)	Evolving Fault or not	Classifier output
1.	AG	-	-	No	1
2.	ABG	-	-	No	2
3.	AG	bg	5	Yes	3
4.	ACG	-	-	No	4
5.	AG	cg	5	Yes	5
6.	ABC	-	-	No	6
7.	AG	abcg	5	Yes	7

8.	AG	bg	10	Yes	3
9.	AG	cg	10	Yes	5
10.	AG	abcg	10	Yes	7
11.	AG	bg	15	Yes	3
12.	AG	cg	15	Yes	5
13.	AG	abcg	15	Yes	7

Table 4.18 shows the results of evolving fault events classification results obtained by the proposed EMD and PNN based approach during testing. The PNN based classifier model is also well effective in ascertaining the evolving events in the compensated transmission network. Figure 4.18 shows the corresponding confusion matrix obtained during testing.

Table 4.18 Evolving fault events classification percentage obtained by PNN based scheme

Fault type	Number of test samples	Number of incorrect classification	Correct classification	Over all Accuracy (%)
AG	600	0	600	100
ABG	600	0	600	100
AG-bg (evolving event)	600	0	600	100
ACG	600	0	600	100
AG-cg (evolving event)	600		600	100
ABC	600	0	600	100
AG-abcg (evolving event)	600	0	600	100

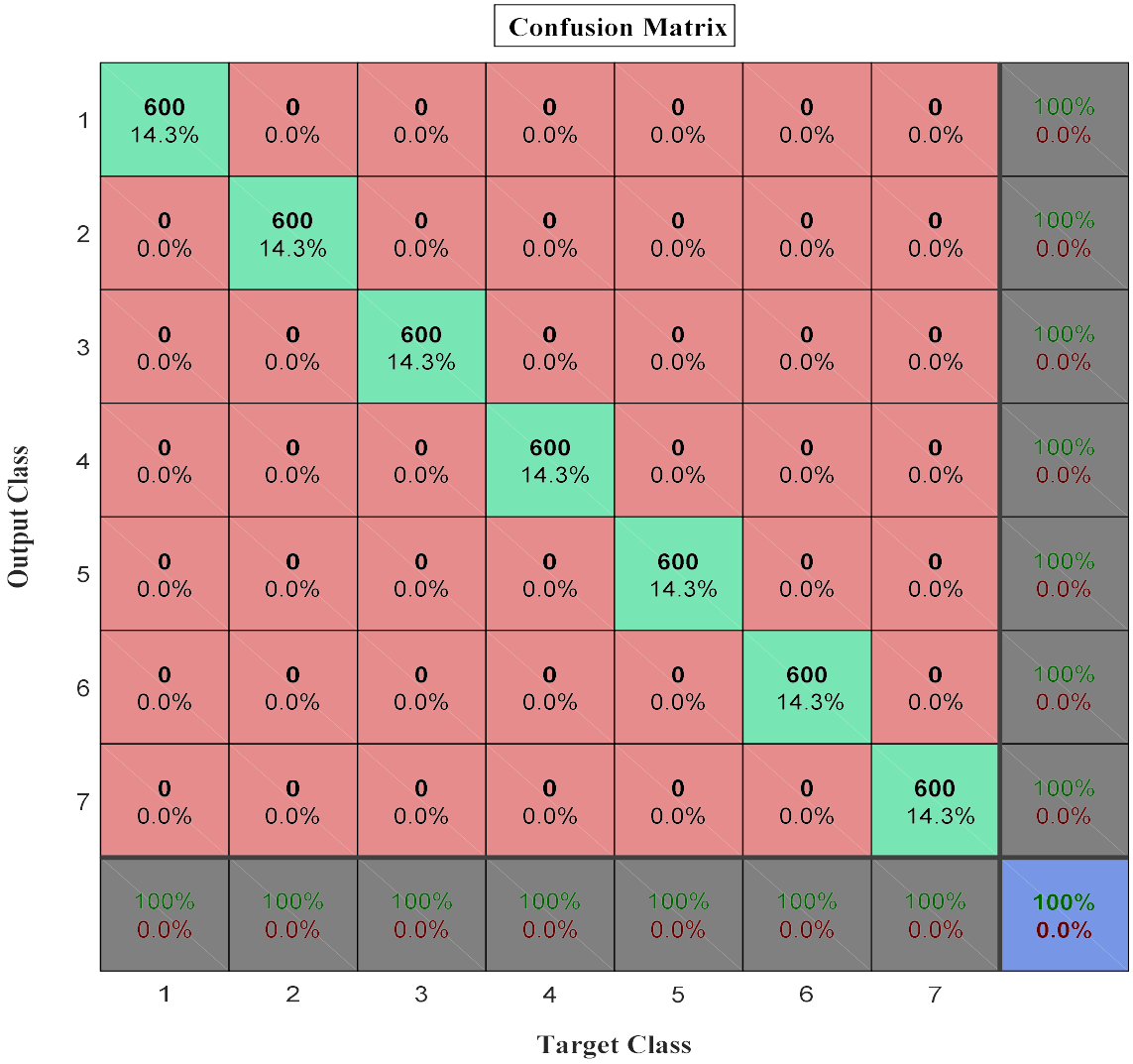

Figure 4.18 Confusion matrix during classification of evolving fault events

4.5 Conclusion

The methodology of empirical mode decomposition and ML classifier based approach for ascertaining the fault events in the compensated power network is presented in this chapter. The work-flow, training and testing procedures of the proposed approach are thoroughly explained. Further, the feasibility and competency of the proposed EMD events ascertaining methodology is analyzed for various fault scenarios on two distinct simulated

test networks. In addition, the performance of the proposed scheme is also evaluated for transforming fault events. By observing the obtained results for various considered testing cases, it has been reaffirmed that the proposed scheme is good enough in ascertaining the fault events in any series compensated power network irrespective of varying fault scenarios.